



Stress-strain behavior in compression of lightweight fiber reinforced concrete under monotonic and cyclic loads

G. Campione, L. La Mendola

*Dipartimento di Ingegneria Strutturale e Geotecnica, Università,
Viale delle Scienze, Palermo, Italy*

Abstract

Compressive experimental behavior of lightweight fiber reinforced concrete combined with traditional transverse steel reinforcement consisting in steel spirals was analyzed. Lightweight aggregates were utilized to give lightness to the composite, and steel hooked fibers were added to the matrices besides the traditional steel lateral reinforcement to increase the ductility of members in compression. The investigation was carried out through compressive tests on cylindrical specimens, by imposing monotonic or cyclic displacements and recording the full load-deformation curves. Empirical stress-strain equations were adopted to reproduce with a good level of approximation the actual behavior of cylindrical specimens under uniaxial compression loads, considering the coupled effect of fibers and steel transverse reinforcement.

1 Introduction

The rapid development of high buildings, larger sized and larger span concrete structures required concrete with good performance in terms of strength, toughness, and light weight, the latter being related to the density of concrete. A decreased density permits a saving in dead load for structural design and foundations, and among other things permits a reduction in the horizontal inertia actions on structures in seismic regions.

With respect to normal weight concrete, lightweight concrete shows more brittleness with an increase in strength level in compression; moreover, the stress-strain curve exhibits linear behavior, with lower stiffness, up to a stress



value which is very close to the maximum strength, and a steeper softening branch. However, the brittleness of lightweight concrete, can also be reduced by using higher percentages of lateral reinforcements, as is also done in normal weight concrete [1-4]. Similar effects are also obtained by adding reinforcing fibers to the concrete matrix, as shown in several recent studies [5-8]. Knowledge of the complete stress-strain curves of confined lightweight plain and fiber reinforced concrete is important for design purposes. Several analytical models [9-13] exist for predicting the behavior of confined normal weight and lightweight concrete, but they refer prevalently to the case of a circular cross-section with steel spiral confinement or with fiber reinforced concrete only. Very little information is available regarding the stress-strain curves in compression in the case of coupled steel spirals and fibers in reinforced concrete.

In the present investigation an experimental study based on simple compressive tests emphasizing the favorable effect of fibers and/or steel spirals in lightweight concrete is reported on an analytical model and proposed based on the actual behavior of cylindrical specimens under uniaxial compression loads, allowing one to consider the coupled effect of fibers and steel transverse reinforcement.

2 Experimental procedure

Cylindrical specimens having diameter $d=100$ mm and height $h=200$ mm were utilized to obtain the complete stress-strain curves under uniaxial monotonic and cyclic compression using displacement controlled tests with a slow rate of displacement of 0.2 mm/min. The axial deformations were measured using three digital transducers with a gauge length of 140 mm, as described in [8].

The lightweight concrete mixes were prepared utilising two different types of lightweight aggregates (pumice stone or expanded clay). The mix design of lightweight plain concretes are given in more detail in [8]. In this context L_p denotes a lightweight concrete matrix with pumice stone coarse aggregate, L_c a lightweight concrete matrix with expanded clay coarse aggregate, and N_r a normal weight concrete matrix. The weight density of hardened concrete without reinforcing fibers proved to be 1800, 1640 and 2420 kg/m³ for lightweight concrete with pumice stone, lightweight concrete with expanded clay and normal weight concrete, respectively. Some specimens were also reinforced with steel spirals and/or steel fibers. The confinement spirals were closed circular spirals of 4 mm diameter having effective transverse cross-section area A_s . The circular spirals, at pitches of $s=25$ or 50 mm, corresponded to steel percentages of $\rho=4A_s/(ds)=2.48$ and 1.24%, respectively; and the lateral maximum pressure confinement was $\sigma=2f_y A_s/(ds)=6.45$ and 3.22 MPa, respectively in which a conventional yielding value for the steel spirals was assumed, $f_y=520$ MPa. In the case of fiber reinforced concrete hooked steel fibers, having length $L_f=30$ mm and diameter $\phi=0.5$ mm, were utilised at different percentages. The volume percentages of fibers were 0.5, 1 and 2%, corresponding to fiber amounts of 40, 80 and 160 kg/m³, respectively.

3 Experimental results

The results obtained in the compressive tests carried out on lightweight fiber reinforced concrete specimens are presented below in the form of σ - ϵ curves; the monotonic curves are obtained as averages of the results of three tests. These results allow one to compare the effects of the aggregate type (pumice stone and expanded clay), of the volume percentage of fibers, and of the volumetric ratio of spiral reinforcements.

3.1 Monotonic and cyclic loading of FRC

Fig. 1 shows the monotonic and cyclic responses respectively of the cylindrical specimens in compression, for the three types of concrete matrix considered (with pumice stone, expanded clay, normal-weight coarse) without reinforcing fibers.

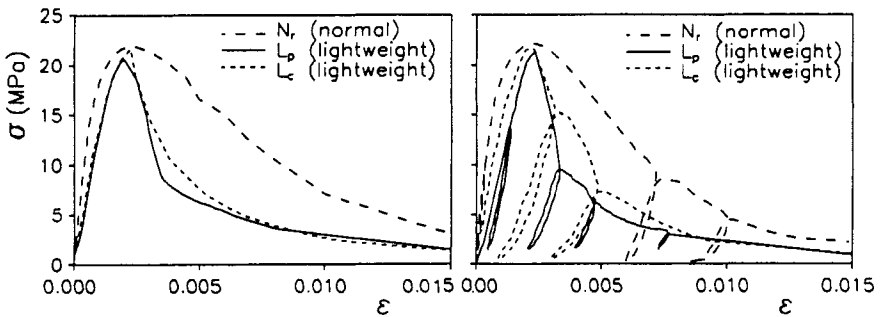


Figure 1: Stress-strain curves for plain concrete.

The shape of the curves shows that lightweight and normal weight concrete exhibit about the same strength, while lightweight concrete is affected by very brittle behavior both with pumice stone aggregates and with expanded clay aggregates. Fig. 2 shows the favorable effect of fibers on the monotonic response in compression of lightweight concrete matrices, in particular in the softening branch.

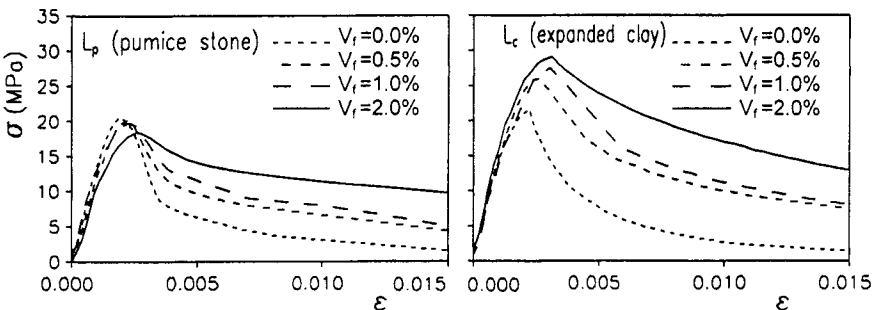


Figure 2: Monotonic stress-strain curves for FRC.



Fig. 3 shows the analogous effect of the fibers on the cyclic response of the lightweight concrete matrices considered. After repeated loading and unloading cycles, lightweight concrete is able to reach significant strength levels even in the softening branch of the response.

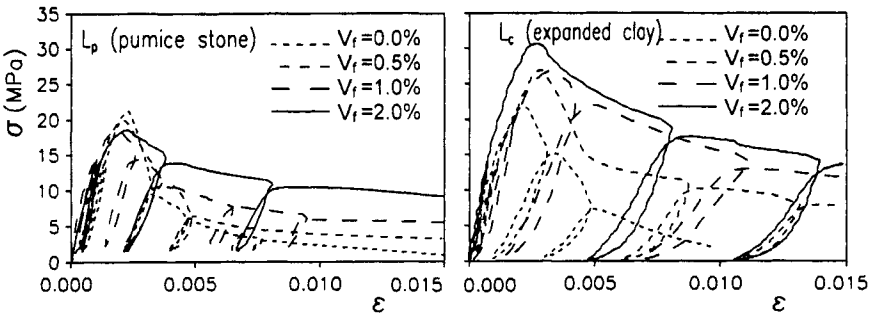


Figure 3: Cyclic stress-strain curves for FRC.

3.2 Monotonic and cyclic loading of FRC with steel spirals

To evaluate the confinement effect of transverse steel reinforcements on lightweight fiber reinforced concrete, compressive tests on cylindrical specimens confined with steel spirals were carried out.

In Fig. 4 the average stress-strain curves for steel spirals and fibers at volume percentages V_f equal to 0 and 1 %, respectively are given.

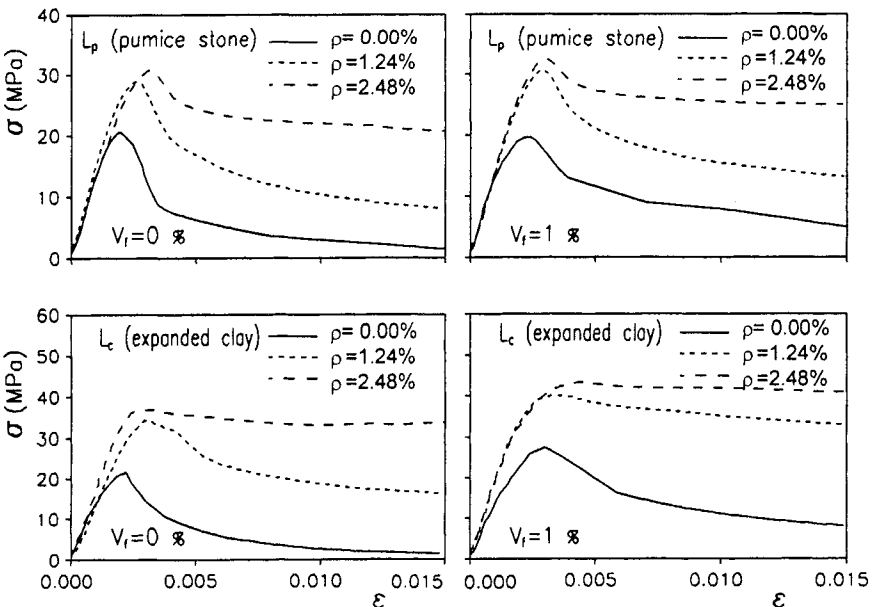


Figure 4: Monotonic stress-strain curves for FRC with spirals.

These results are relative to different percentages of steel spirals with and without fibers. The addition of both fibers and steel spirals produces an increase in the maximum bearing capacity and also in the residual strength with respect to the case of steel spirals or fibers only.

A comparison between the curves obtained in the absence of fibers ($V_f = 0\%$), both for pumice stone and for expanded clay, shows an increase in the bearing capacity of lightweight concrete due to steel spirals.

This effect, however, is lower than that obtained for normal weight concrete when the same percentage of steel spirals is adopted. This is due to the lower lateral expansion of lightweight concrete with respect to normal weight concrete, producing a lower lateral confining pressure, and also to the brittle nature of lightweight aggregate, determining a premature failure of the specimen before the yielding stress in the steel spirals is reached.

In Fig. 5 the cyclic responses of fiber reinforced concrete with steel spirals are represented.

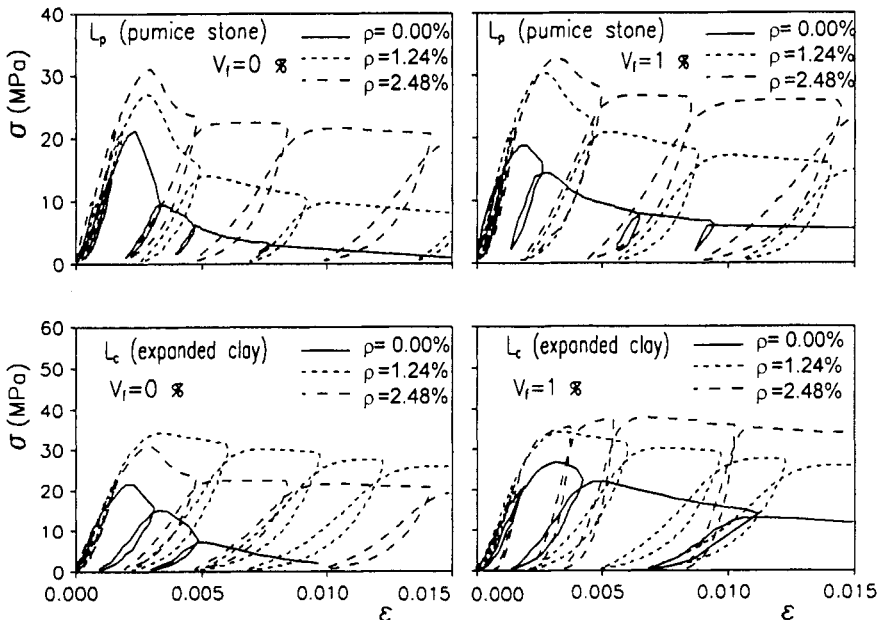


Figure 5: Cyclic stress-strain curves for FRC concrete with spirals.

The coupled use of steel spirals and fibers, as observed for the monotonic response, also ensures high performance under cyclic action. It is interesting to observe that when the materials reinforced with steel spirals in the softening branch were unloaded, lower residual deformations were observed with respect to the case of fibers alone. This is due to the fact that in lightweight concrete with steel spirals the stress in the spirals does not reach the yield value and when specimens are unloaded the elastic elongation in steel spirals is recovered.

4 Analytical stress-strain law

Several empirical stress-strain curves for confined normal and high strength concrete [9-12] have been proposed in the literature; these are based on simple analytical relationships in which the fundamental parameters obtained in compressive tests are the maximum stress, the corresponding strain, the tangent modulus of elasticity etc. Much work has been done on modeling the stress-strain curves in compression for fiber reinforced concrete, both for normal and high strength concretes. The simple analytical models developed allow one to fit the numerous experimental data very well and they only require knowledge of the characteristic values obtained by simple standard laboratory tests; however, these models do not allow one to study the effective micro-mechanical behavior of material, as recently done by mechanical models based on nonlinear fracture mechanics [14].

In the case of lightweight fiber reinforced concrete with pumice stone or expanded clay, brittle behavior is observed, as in high strength concrete; for this reason in the present investigation the stress-strain curves determined experimentally were modeled using the recent relationships proposed by Hsu and Hsu [12] for high strength fiber reinforced concrete. This model is represented in Fig.6 in terms of normalized stresses $x = \sigma / f_c'$ and normalized strains $\eta = \varepsilon / \varepsilon_0$, ε_0 and f_c' being the strain and the stress corresponding to the peak load. The curve exhibits two different branches: - the first one fitting experimental results from zero stress up to coordinate point x_d, η_d and the second one from point x_d, η_d up to the point at which a complete loss of bearing capacity occurs.

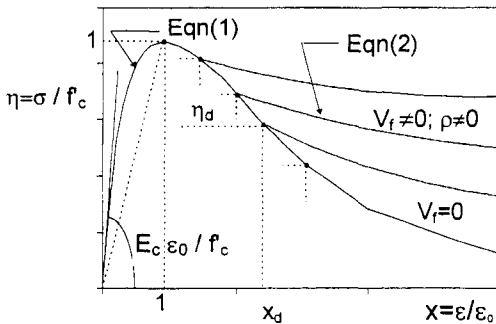


Figure 6: Analytical model.

The following equations are utilized:

$$\frac{\sigma}{f_c'} = \frac{\beta \cdot \frac{\varepsilon}{\varepsilon_0}}{\beta - 1 + \left(\frac{\varepsilon}{\varepsilon_0}\right)^\beta} \quad 0 \leq \frac{\varepsilon}{\varepsilon_0} < x_d \quad (1)$$

$$\frac{\sigma}{f'_c} = \eta_d \cdot \exp \left[-k_d \cdot \left(\frac{\varepsilon}{\varepsilon_0} - x_d \right)^\alpha \right] \quad \frac{\varepsilon}{\varepsilon_0} \geq x_d \quad (2)$$

with reference to the symbols in Fig. 6; β is a parameter modeling the slope of the ascending branch depending on the type of concrete (plain, fibrous or confined); x_d and η_d are the coordinates of the point at which the change in the equations occurs; Hsu and Hsu [12] assume η_d to be a share of the maximum stress f'_c ; in the present study this dimensionless stress value is assumed to vary with the volume percentages of fibers and with the volumetric percentages of steel spirals. In the model, k_d and α are two parameters governing the shape of the softening branch.

4.1 Characteristic parameters of the constitutive law

In the present section the fundamental parameters of Eqs. (1) and (2) are related to the volume percentage of fiber V_f and to the volumetric ratio of steel spirals ρ . The analysis was carried out determining the parameter giving the best fitting results in accordance with experimental data and then an analytical law was proposed by adopting a regression analysis.

According to the experimental data the parameter β can be assumed to vary linearly with V_f for a fixed value of ρ and also with ρ for a fixed volume of fibers V_f . It is interesting to observe that β changes significantly with an increase in V_f , in the case of both pumice stone and expanded clay. In order to explain the variation in the β values it can be observed that in the model proposed by Mander et al. [9] this parameter is expressed by the following ratio:

$$\beta = \frac{E_c}{E_c - \frac{f'_c}{\varepsilon_0}} \quad (3)$$

Increasing the confining level due to the presence of fibers, for a fixed value of ρ , it was observed that in the case of pumice stone β decreases because the initial tangent modulus E_c does not change significantly, while the secant modulus f'_c/ε_0 decreases; the latter decrease is due to the fact that when ε_0 increases significantly the peak stress f'_c does not change in the same way; analogous considerations can be made in the case of expanded clay.

In the case of an increase in confinement due to the steel spirals in the fibrous concrete, for a fixed value of V_f , the following observations are valid: - in the case of pumice stone β increases because E_c does not change significantly, while more strength capacity is achieved involving an increase in f'_c/ε_0 ; - in the case of expanded clay β decreases because ε_0 increases more significantly with respect to f'_c . On the basis of the experimental results it appears reasonable to relate the β coefficient with V_f and ρ with the following expressions:

394 *Earthquake Resistant Engineering Structures III*

$$\beta = (-63.43 + 806.45 \cdot \rho) \cdot V_f + 3.58 + 20.16 \cdot \rho \quad \text{for pumice stone} \quad (4)$$

$$\beta = (-80.86 - 100.80 \cdot \rho) \cdot V_f + 3.65 - 24.19 \cdot \rho \quad \text{for expanded clay} \quad (5)$$

The parameter α models the concavity of the softening branch of the response and it was observed that it was constant with the variation in the volume percentage V_f and in the volume percentage of steel spiral ρ and in what follows it is assumed 0.55 and 0.70 for pumice stone and expanded clay, respectively.

The k_d parameter governs the slope of the softening branch. For pumice stone it exhibits a reduction with V_f and ρ as follows:

$$k_d = (-16.00 - 665.32 \cdot \rho) \cdot V_f + 0.5 - 16.13 \cdot \rho \quad (6)$$

For the case of expanded clay in the absence of steel spirals a linear reduction with V_f is observed:

$$k_d = -9.20 \cdot V_f + 0.47 \quad (7)$$

and in the presence of spirals a constant value equal to 0.05 can be assumed.

It can be observed that a decrease in the k_d values corresponds physically to an increase in the confining level in lightweight concrete.

In the case of pumice stone this variation is sensitive to the effect of the volume percentage of steel spiral and fibers, while in the case of expanded clay this effect is independent of the increase in steel spirals. When a very high volume percentage of spirals is utilized the slope of the softening branch is practically horizontal ($k_d=0.05$) and hence independent of V_f and ρ .

The η_d parameter represents the stress ratio (referred to f_c') corresponding to the attachment point of the two branches of the stress-strain curves expressed by Eqs. (1) and (2), and physically represents the load level at which the localization of the cracks in the specimen occurs, and the fibers bridge the cracks, aiming to the matrices higher residual strength. Obviously with an increase in the volume percentage of fibers these levels of stress increase but no significant reduction in maximum strength is observed up to very high strain values. In the case of pumice stone an increase in η_d values with V_f and ρ is observed and good results in agreement with experimental data are obtained using the following:

$$\eta_d = (14.25 - 306.47 \cdot \rho) \cdot V_f + 0.52 + 12.34 \cdot \rho \quad (8)$$

In the case of expanded clay in the absence of transverse reinforcement a linear increase with V_f can be assumed:

$$\eta_d = 22.74 \cdot V_f + 0.51 \quad (9)$$

and in the presence of steel spirals a value not depending on V_f can be assumed: $\eta_{fd}=0.94$ for $\rho=1.24\%$ and $\eta_{fd}=0.98$ for $\rho=2.48\%$.

In Fig. 7 a comparison is shown between the analytical stress-strain curves and the experimental average curves. It can be observed that the model performs very well in all cases, giving a good level of approximation.

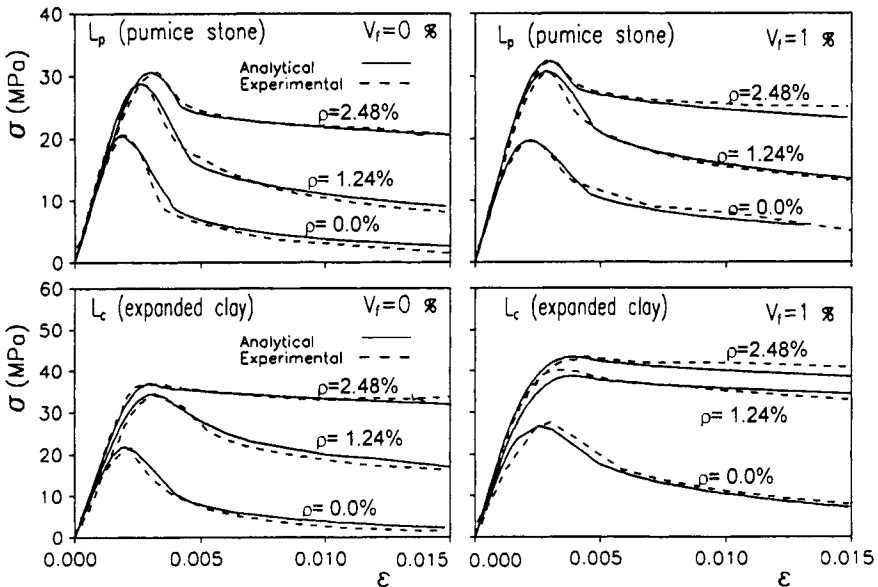


Figure 7: Analytical model for stress- strain curves for confined FRC.

5 Conclusions

Based on compressive tests on cylinders of lightweight fiber reinforced concrete in the presence of steel spirals, the following conclusions can be drawn:

1. Very brittle behavior of lightweight concrete in the case of both pumice stone and expanded clay under monotonic and cyclic loads is observed.
2. The addition of fibers increases the residual strength and the energy absorption capacity; for expanded clay it produces an increase in the bearing capacity up to 30 %, while for pumice stone no significant variation is observed.
3. In the case of both pumice stone and expanded clay a significant increase in energy absorbed as measured by the toughness indices is obtained.
4. In the presence of fibers, concrete reinforced with steel spirals shows an increase in the strength and corresponding strain and in the energy absorbed compared to plain concrete confined by steel spirals alone.
5. The analytical model proposed, based on knowledge of standard parameters obtained using compressive tests, is able to take into account the beneficial effect of fibers and steel spirals and agrees very well the experimental results.



References

- [1] Martinez, S., Nilson, A.H. & State F.O. Spirally reinforced high-strength concrete columns. *ACI Journal*, Proceedings, **81(9)**, pp. 431-442, 1984.
- [2] Mander, J.B., Priestley, M.J.N. & Park, R. Observed stress-strain behaviour of confined concrete. *Journal of Structural Engineering, ASCE*, **114(8)**, pp. 1827-1849, 1988.
- [3] Sheikh, S.A., & Toklucu, M.T. Reinforced concrete columns confined by circular spirals and hoops. *ACI Structural Journal*, **90(5)**, pp. 542-553, 1993.
- [4] Nuti C. & Pinto, P.E. Impiego del calcestruzzo leggero strutturale in zone sismiche. *L'Industria Italiana del Cemento*, **7-8**, pp. 516-528, 1994.
- [5] Balaguru, P. & Foden, A. Properties of fiber reinforced structural lightweight concrete. *ACI Structural Journal*, **93(1)**, pp. 62-78, 1996.
- [6] Campione, G., La Mendola, L. & Zingone, G. Strength and ductility of high strength fibre reinforced concrete circular columns subjected to eccentric loads. *11-th European Conference Earthquake Engineering*, Parigi, Abstract volume p. 154, CD-rom T2/12, 1998.
- [7] Campione, G., Mindess, S. & Zingone, G. Compressive stress-strain behavior of normal and high-strength carbon-fiber concrete reinforced with steel spirals. *ACI Materials Journal*, **96(1)**, pp. 27-34, 1999.
- [8] Campione, G., Miraglia, N. & Papia, M. Mechanical properties of steel fibre reinforced lightweight concrete with pumice stone or expanded clay, *Materials and Structures*, **34(238)**, pp.201-210, 2001.
- [9] Mander, J.B., Priestley, M.J.N. & Park, R. Theoretical stress-strain model for confined concrete. *Journal of Structural Engineering, ASCE*, **114(8)**, pp. 1804-1826, 1988.
- [10] Cusson, D. & Paultre, P. Stress-strain model for confined high-strength concrete. *Journal of Structural Engineering, ASCE*, **121(3)**, pp.468-477, 1995.
- [11] Attard, M.M. & Setunge, S. Stress-strain relationship of confined and unconfined concrete. *ACI Materials Journal*, **93(5)**, pp. 432-443, 1996.
- [12] Hsu, L. S. & Hsu, C.T.T. Stress-strain behavior of steel-fiber high-strength concrete under compression. *ACI Structural Journal*, **91(4)**, pp. 448-457, 1994.
- [13] Khaloo, A.R., El-Dash, K.M. & Ahmad, S.H. Model for lightweight concrete columns confined by either single hoops or interlocking double spirals. *ACI Structural Journal*, **96(6)**, pp. 883-890, 1999.
- [14] Bazant, Z.P. & Planas, J. Fracture and size effect in concrete and other quasi brittle materials. CRC press LLC, Boca, Raton, Boston, London, New York, Washington, D.C., 616 pp., 1998.